UDC 533.9
IRSTI 29.27.35

https://doi.org/10.55452/1998-6688-2026-23-3-388-397

[1]***Tazhen A.B.,**
PhD, ORCID ID: 0000-0002-3277-2086,
*e-mail: Aigerim@physics.kz
[1]**Kholmirzayev A.N.,**
PhD student, ORCID ID: 0009-0003-4108-0879,
e-mail: kholmirzayev.abdulla@gmail.com
[2]**Ussenov Y.A.,**
PhD, ORCID ID: 0000-0001-7903-8674,
e-mail: yerbolat@physics.kz
[1]**Dosbolayev M.K.,**
Cand. Phys. Math. Sc., Prof., ORCID ID: 0000-0002-0724-1793,
e-mail: merlan@physics.kz
[1]**Ramazanov T.S.,**
Dr. Phys. Math. Sc., Prof., ORCID ID: 0009-0009-2301-1152,
e-mail: ramazan@physics.kz

[1]National Nanotechnology Laboratory of Open Type, al-Farabi Kazakh National University, Almaty, Kazakhstan
[2]Princeton Plasma Physics Laboratory, Princeton University, Princeton, USA

STUDY OF CHANGES IN MICROHARDNESS AND MASS OF A PREHEATED TUNGSTEN UNDER THE INFLUENCE OF PULSED PLASMA

Abstract

The paper presents the results of an experimental investigation of changes in the microhardness and mass of a preheated tungsten target, the primary candidate material for the first wall and divertor, subjected to a pulsed plasma flow of approximately 0.2 ms duration. The experiments were conducted as a series of 13 pulses, each with an energy density and power density of approximately 1.1 MJ/m^2 and 5.5 GW/m^2, respectively. Microhardness was measured using an HVS-1000B hardness tester; the target mass before and after plasma exposure was measured using a CPA225D precision balance. It is shown that the microhardness of the tungsten target remains virtually unchanged even at the maximum irradiation dose (up to 39 pulses), and the observed change is within the measurement error, which indicates the structural stability of the surface layer. At the same time, an increase in the target mass (up to 31 mg) was recorded, probably caused by contamination and redeposition of the material of external structural components. Energy-dispersive spectroscopy (EDS) analysis revealed Cu, Zn, Ni, and C lines in dust particles redeposited on the target surface. The results indicate that these foreign components have a significant impact on surface morphology and should be considered when interpreting tungsten damage mechanisms.

Key words: pulsed plasma accelerator, plasma flow, preheated tungsten target, microhardness, target mass, elemental composition of the target.

Received May 08, 2026; revised July 07, 2026; accepted July 10, 2026.

Introduction

Despite the large number of experimental studies conducted on simulation facilities and operating tokamaks, the study of plasma interactions with materials has not lost its relevance and continues to attract the attention of researchers due to the construction of experimental fusion reactors such as

ITER and DEMO [1–5]. In the conditions of high-density, high-temperature fusion plasma, materials in contact with plasma are expected to experience extreme plasma-thermal loads [6, 7]. According to the technical characteristics of the ITER reactor, beryllium (Be) was selected as the metallic material for the armor of the first wall due to its low atomic number Z [8]. However, in early 2025, ITER reconsidered the use of beryllium due to potential risks associated with its toxicity and high erosive properties [9]. The latest update to the technical solutions of the ITER project includes replacing the beryllium wall with a tungsten one [10]. This solution meets the stringent requirements for materials in contact with plasma. First, the material must have high strength and structural stability under extreme operating conditions.

Tungsten is known to be the most refractory of metals; however, it is vulnerable to plasma exposure. When plasma interacts with a tungsten target, a change in the surface properties is observed, followed by a change in the target mass [11–13]. This may be due to structural changes in the material. In this regard, a significant number of microstructural studies have been conducted to understand the response of different types of tungsten to plasma and other types of irradiations (e.g. laser, etc.). It was found that the average surface hardness of the initial target made of a heavy tungsten alloy decreases at the initial level of the plasma beam power density (0.108 MW/m^2). An increase in power density by 1 MW/m^2 is accompanied by a linear increase in the average surface hardness. In [14], it is shown that this effect is due to an increase in the density of dislocation lines. In [15], the change in microhardness in tungsten monoblock samples was investigated as a function of the heat flux penetration depth at a power density of 10 MW/m^2. As follows from [15], no noticeable changes were observed inside the tungsten before and after exposure to a heat flux (at a depth of 200 μm to 6.8 mm); however, a noticeable decrease in mechanical strength was observed near the surface, manifested in a decrease in hardness. The results presented in [16] indicate an insignificant decrease in the microhardness of the surface layer of a single-crystal tungsten sample (up to 15% after irradiation with pulsed helium plasma flows using the Vikhr facility). According to the authors, this is due to the formation of a crystallization texture in the surface layer. Analysis of these data allows us to conclude that pure tungsten is characterized by structural instability in the plasma thermal impact zone. This is reflected in the hardness of this material. Several studies [17–19] have examined in detail the methods for increasing the hardness of tungsten materials in contact with plasma using additives such as carbon, yttrium oxide, and some metals (Ni, Co, Cr) characterized by appropriate ductility and high-temperature strength.

The paper presents the results of an experimental study of changes in the microhardness and mass of a preheated tungsten target depending on the number of plasma pulses.

Materials and methods

A PW-7 pulsed plasma accelerator was used as a source of plasma flow for irradiating a preheated tungsten target [20, 21]. The accelerator was equipped with coaxial copper electrodes separated by an insulator [22]. A bank of capacitors with a total capacitance of 1.4 mF and charged to a voltage of 5 kV was connected to an RVU-43 vacuum spark gap. A Rogowski coil was installed around the current-carrying part of the plasma accelerator to measure the discharge current. The maximum value of the discharge current reached approximately 100 kA. In the experiments under consideration, the tungsten target was exposed to hydrogen plasma with the following parameters: electron temperature $T_e \approx 23\text{-}40$ eV and charged particle concentration $n_e \approx 10^{15}$ cm^{-3} [22, 23]. The plasma flow velocity in the accelerator varied in the range of $10^4 - 3\cdot10^4$ m/s [24, 25].

A 1.5 × 1.5 cm^2, 2 mm thick plate made of high-purity (99.96%) hot-rolled polycrystalline tungsten was used as a target. The average grain size, determined from scanning electron microscope (SEM) images, is approximately 2 μm. The target was located 22 cm from the electrode system. The surface of the tungsten plate was polished mechanically and electrochemically using abrasive paper and a KOH solution. Irradiation was carried out in three series of 13 plasma pulses each, with a peak energy density of 1.1 MJ/m^2 and a pulse duration of about 0.2 ms [20]. In this study, a tungsten sample was exposed to a relatively small number of pulses. This value was chosen taking into account the aim of this study, which was to investigate the initiation stage of tungsten damage under the influence of thermal loads similar to ELM discharges. A special holder with a preheating system was used to position the tungsten plate inside the vacuum chamber [21]. The heating system included a thick tantalum plate (40 µm thick) heated by an electric current passing through conducting contacts. A heat-resistant ceramic insulator was installed between the tantalum and tungsten plates. Before and during plasma irradiation, the tungsten plate temperature was maintained at 823 K, ensuring conditions above the ductile-to-brittle transition temperature. This temperature regime was maintained between experimental series with a tolerance of ±41 K. A type K (chromel-alumel) thermocouple was used for temperature control. Before starting the operation, the vacuum chamber was evacuated to a pressure of 10^{-4} Torr using a pre- and diffusion pump. The chamber was then filled with working gas. When a control voltage pulse was applied between the main and the trigger electrodes of the spark gap, the gas in the interelectrode gap ionized and accelerated toward the target. Plasma streams irradiated the surface along their normal, as shown in Figure 1.

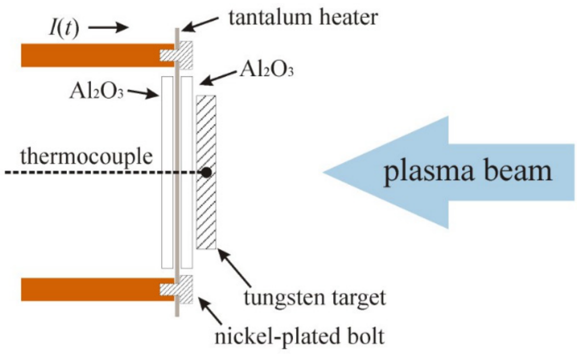

Figure 1 – Schematic diagram of the setup for plasma irradiation of a tungsten target [21]

The microhardness of the irradiated surface of the tungsten plate was measured by the Vickers method using a Vickers hardness tester HVS-1000B. The measurement error along the indentation diagonal was δd = ±0.2 µm. The microhardness measurement error was calculated taking into account the spread of the measurement error along the diagonal indentation and determining using the formula , which was no more than 1%. To measure the mass of the tungsten plate, a CPA225D precision scale with an accuracy of δm = ±0.01 mg was used. Energy-dispersive spectroscopy (EDS) was used to determine the chemical composition of the tungsten plate.

Results and discussion

Under operating conditions in a fusion reactor, the materials of the first wall and divertor are subjected to extreme plasma and thermal loads. Under these conditions, microhardness is a key parameter determining the performance and durability of candidate materials, as it is directly related to resistance to plastic deformation, erosion, cracking, and surface degradation. Microhardness changes under repeated plasma pulses reflect the evolution of the material's structure, including hardening, recrystallization and defect accumulation. The dependence of tungsten target microhardness on the number of plasma and thermal loads exposures is shown in Figure 2. Before and after irradiation, 10 microhardness measurements were performed in each case. Figure 2 shows the mean values and corresponding standard deviations.

Before irradiation, the microhardness of the tungsten target was 514.8±5 HV, which corresponds to a hardened state of the material compared to annealed tungsten. As shown in Figure 2, in all three series of irradiation with different numbers of pulses (13, 26 and 39), the microhardness value changes within the measurement error (≈ 0.0027 – 0.0056 ≈ 0.27-0.56 % ($\Delta HV_1 = HV_0 - HV_{13} =$

1.4 HV change towards increase, $\Delta HV_2 = HV_0 - HV_{26} = 0$ HV, $\Delta HV_3 = HV_0 - HV_{39} = 2.9$ HV change towards decrease) and does not indicate any significant changes in the mechanical properties of the tungsten target.

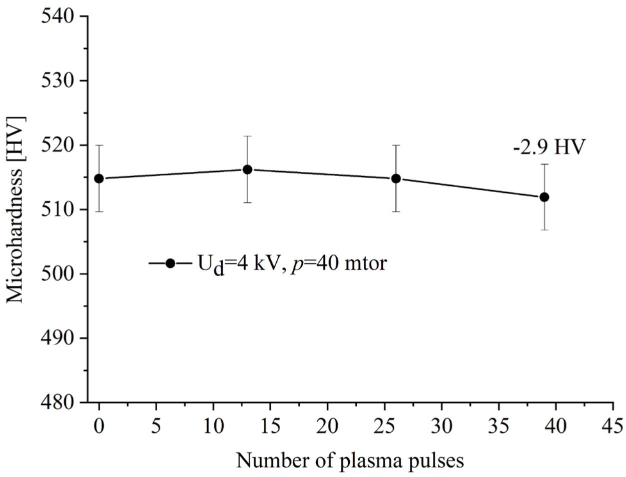

Figure 2 – Microhardness values of a tungsten target before and after irradiation

An analysis of the surface morphology using scanning electron microscopy has previously shown [21] that exposure to pulsed plasma flows leads to the formation of cracks on the surface of a tungsten target. This result indicates the localized internal residual stresses in the near-surface layer. Despite this, no increase in microhardness was observed. The crack thickness was very small – up to several hundred nanometers. This indicates insignificance of local stresses. Consequently, stresses are likely effectively redistributed during target cooling and, thus, have no noticeable effect on microhardness. It has previously been experimentally demonstrated [20, 21] that the crack size on the surface of a tungsten target does not change significantly with increasing pulse number. This effect was observed under controlled temperature conditions, such that the minimum initial temperature of the backside of the tungsten target does not fall below a specified value, T_{DBTT}. This result indicates that with increasing irradiation dose, residual stress between the irradiated layer and the preheated part of the target do not tend to increase further but rather tend to relax. Thus, the observed behavior qualitatively explains the experimental microhardness data. It should be noted that the Vickers indentation size is several tens of micrometers (42–43 μm), while the observed crack openings are significantly smaller. Consequently, the measured microhardness may be determined primarily by the properties of the surrounding material, and the contribution of localized surface defects may be insufficient to detect statistically significant changes.

The results of microhardness measurements were compared with the data presented in [14–16]. In contrast to studies that reported changes in the microhardness of the subsurface layer of tungsten after cyclic exposure to an electron beam and plasma, this study revealed no significant changes in microhardness after repeated exposure. This is explained by the specific conditions under which the tungsten studies were conducted. It should be noted that the temperature regime used in our experimental conditions leads to a change in the response of tungsten to plasma exposure. The observed discrepancies between the present results and the data from [14, 15] are also explained by variations in the irradiation parameters. In [14], tungsten targets were continuously irradiated for 15 min, whereas in [15], tungsten monoblock mock-ups were irradiated with approximately 5000 cycles, each with a duration of 10 s followed by a 10 s cooling interval. The tests were conducted at power densities of 1 and 10 MW/m^2. It should be noted that the aim of [15] was distinct from that of the present study. That study focused on tokamak operation in the long pulse mode, where the plasma exposure is very similar to the annealing process. In contrast, this study examines significantly shorter pulses that produce thermal shock effects. Consequently, the present work revealed loss of crystallinity and grain fragmentation, whereas in [15], the repeated heating and cooling cycles likely contributed to reorganization of the microstructure, gradual coarsening of grains and, as a result, a decrease in microhardness. Furthermore, cooling of the tungsten monoblocks is an inherent aspect of the tokamak operating conditions and was probably one of the factors taken into account by the authors [15]. In terms of the impact parameters, the study [16] is the closest to the present study; it also reports a slight decrease in the microhardness of the tungsten surface layer (up to 15%). The authors interpret this effect to radiation-thermal remelting of the surface layer and subsequent directional solidification. During cooling, a crystalline texture is formed, oriented along the temperature gradient, which is accompanied by microstructural rearrangement and partial relaxation of accumulated defects.

Although a complete comparison of the results is impossible due to differences in the experimental conditions, the data obtained indicate that the temperature regime implemented in this study, as in [16], creates favorable conditions for the relaxation of defects and internal stresses. This is consistent with the fact that at temperatures above the DBTT, the mechanical properties of tungsten change significantly, which may contribute to the retention of microhardness after repeated exposure.

Exposure to pulsed plasma flows significantly affects the surface of the material being processed, leading to changes in surface morphology. As shown in [26, 27], short plasma pulses can cause tungsten melting, leading to ablation, accompanied by mass loss in the samples. The main contribution to this process is erosion caused by the ejection of molten droplets and solid fragments of the material. The dependence of the change in tungsten target mass on the number of plasma irradiations is shown in Figure 3. The following pattern was observed: after 13, 26, and 39 pulses, a steady increase in target mass was observed. After 39 pulses, the tungsten target mass increased by Δm_{39} = +31 mg compared to the initial value. Considering the measurement error of the electronic scale, this change can be considered a reliable quantitative result. The observed mass increase may be due to the deposition of erosion products and redeposition of material in the target's near-surface layer, indicating a complex balance between erosion and redeposition processes under pulsed plasma exposure.

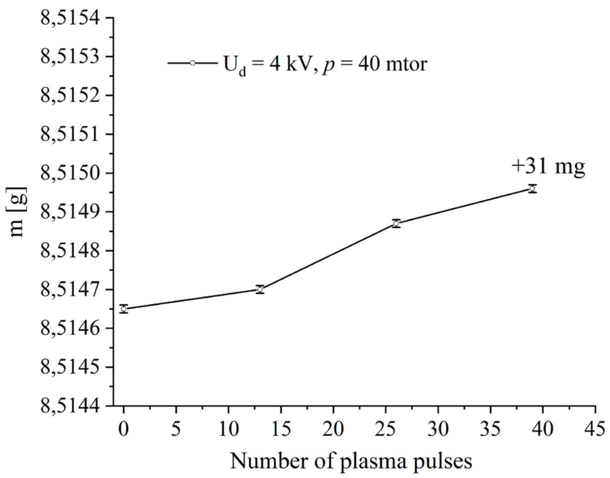

Figure 3 – Dependence of the mass of
a tungsten target on the number of plasma exposures

Accordingly, this can be explained by the fact that impurity transport and deposition of impurities on the surface by the plasma flow, together with the above-mentioned processes, strongly influence the observed behavior. Figure 4 shows an image of a target surface area after exposure to pulsed plasma, obtained using a scanning electron microscope, as well as the results of energy-dispersive spectroscopy (EDS) analysis of the localized area highlighted in the micrograph.

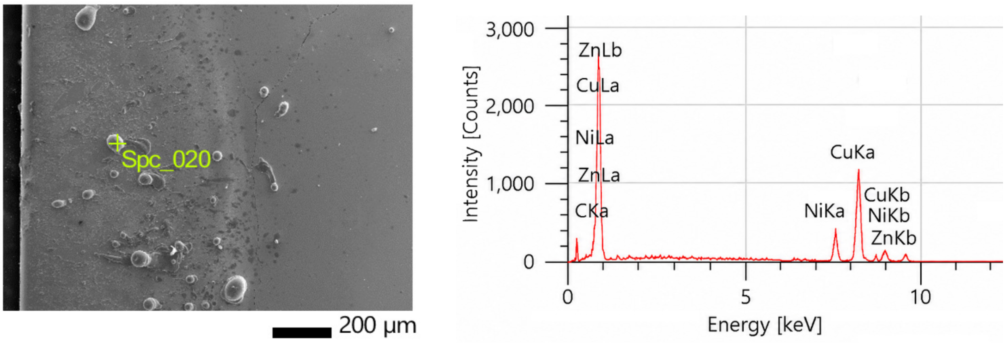

Figure 4. a) SEM image of the surface of a tungsten target after 39 irradiations, b) elemental composition of the area indicated in the SEM image

It should be mentioned that the analyzed area is situated near the sample holder, so this must be taken into account when interpreting the elemental composition of the surface. On the irradiated surface of the tungsten plate, numerous spheroidal formations are observed, having the morphology of solidified drops of molten metal. The size of these particles in the analyzed region is approximately 40–45 μm. The shape of these particles may indicate the following process: the material melted during the discharge, was then transferred to the target surface, and solidified into droplets. The obtained EDS spectrum of the analyzed local region containing these particles reveals intense Cu, Zn, and Ni lines, as well as a weak C peak. The presence of copper, zinc and nickel indicates that the observed droplets are associated not only with processes occurring within the tungsten target itself, but also with the transfer of material from the components of the holder or other structural elements of the experimental setup. Thus, the observed change in the mass of the tungsten plate is likely due to local heating, melting and sputtering of materials, followed by the deposition of metallic particles onto the tungsten surface during plasma exposure. However, the obtained results do not allow us to unambiguously determine the origin of the detected particles, although they indicate the possible involvement of additional sources of material in addition to the tungsten target. Although plasma exposure typically results in surface erosion, in this case, the contribution of redeposited material may partially offset or even exceed the mass of tungsten removed. This is particularly likely for areas located close to the holder, where the probability of melted or evaporated structural material particles depositing on the target surface is higher. The mass of deposited droplets can be approximately estimated by assuming them are spherical particles. The average diameter of clearly visible spherical droplets of molten metal is approximately 40-45 μm. The mass of a single spherical particle is estimated at 0.3-0.4 μg, given a metal density of approximately 8.5-8.9 g/cm^3. These particles are localized in significant quantities around the metal holder on both sides of the tungsten target. As shown in Figure 4a, the particle density in the region under investigation is approximately 14.6 particles/mm^2. The obtained estimate suggests that at such a particle density, their contribution to the observed mass increase may be insufficient to explain the measured mass increase. It should be noted that this estimate is approximate. In addition, the calculations were carried out assuming a uniform distribution of particles over the sample surface.

Since energy-dispersive spectroscopy (EDS) analysis does not allow direct assessment of the distribution of detected impurities across the entire surface of the tungsten plate, it is impossible to quantify their contribution to the change in sample mass. Therefore, the presence of redeposited particles is considered only as one possible factor in the observed mass increase. Furthermore, based on the quantitative estimates obtained, it seems inappropriate to attribute the observed mass increase solely to the deposition of the detected particles, as the mass increase may also be due to small particles, redeposited layers of material, or the uneven distribution of redeposition products, which are not accounted for in the local surface analysis. Thus, the SEM/EDS analysis results indicate the presence of redeposited particles on the surface of the tungsten plate. In addition to erosive surface modifications, the contribution of material transfer from the experimental system components should be considered. This must be taken into account when analyzing the mass balance of the tungsten plate, as the mass increase after irradiation may be due not to changes in the tungsten itself, but to the deposition of molten metal particles originating from the structural components.

As shown in a previous study [31], bubbles, craters, and remelting zones were observed on the tungsten surface. Such defects may have a localized impact on the mechanical properties of the material. It should be noted that microhardness measurements were not conducted directly in areas exhibiting morphological features. A correlation between surface morphology and microhardness cannot be ruled out. To confirm this, further research is needed, including a comparison of localized microhardness measurements in the areas of the defects.

Conclusion

In this work, experimental studies were carried out on changes in the microhardness and mass of a preheated tungsten target after exposure to plasma pulses with a duration of about 0.2 ms. To obtain more complete information on changes in the initial properties (including microstructural characteristics, etc.) of the irradiated target, experiments were conducted in several series with different plasma doses, each series including 13 intense plasma pulses (approximately 5.5 GW/m^2). The experiments showed that microhardness remains virtually unchanged even at the highest irradiation dose. After 39 pulses, a minor change in microhardness 2.9 HV is observed, consistent with the measurement accuracy of the measuring instrument. Taking into account the above, the results show that the structural stability of the surface layer of the preheated tungsten target is maintained. At the same time, some data from our previous experimental work, such as the absence of change in crack opening from pulse to pulse and the slight change in stresses in the near-surface layer of the tungsten target (indicating relaxation), provide an explanation. When measuring the mass of the tungsten target, an increase was detected; the mass increase after 39 pulses was 31 mg. The obtained results demonstrate that erosion products from the experimental system components, as well as carbon-containing impurities (including vacuum oil vapor), penetrated the tungsten surface layer. This is confirmed by scanning electron microscopy (SEM) data, which revealed the presence of dust-like particles, and energy-dispersive spectroscopic analysis (EDS), which revealed the presence of Cu, Zn, Ni, and C impurities. Thus, the observed increase in the mass of the tungsten plate can be explained by the redeposition of foreign material on the sample surface. When analyzing tungsten surface damage caused by pulsed plasma, it is important to consider the presence of impurities in the plasma flow. The origin of the detected impurities has not been definitively established; possible sources include erosion products of experimental system components, residual gas components, and carbonaceous contaminants. These may affect the condition of the surface layer of the tungsten target. The presence of such impurities can lead to the formation of redeposited layers, changes in the elemental and phase composition of the surface, and redistribution of heat and mass transfer processes in the near-surface region. Therefore, the observed defects, including cracks, bubbles, craters, and localized melting zones, cannot always be unambiguously attributed solely to plasma thermal shock, as their formation can be further determined by the influence of impurity components on gas accumulation, erosion, and structural degradation of the material. Thus, when interpreting experimental results, the impurity composition of the plasma flow should be considered as one of the significant factors influencing the mechanisms and degree of damage to tungsten.

Funding

This work was funded by the Ministry of Science and Higher Education of the Republic of Kazakhstan (project No. IRN AP23490402).

REFERENCES

1 Loarte, A., Pitts, R.A., Wauters, T., Nunes, I., Vries, P. de, Kim, S.H., Köchl, F., Polevoi, A., Lehnen, M., Artola, J. The new ITER baseline, research plan and open R&D issues. Plasma Phys. Control. Fusion, 67, 065023 (2025). https://doi.org/10.1088/1361-6587/add9c9

2 Komm, M., Jaulmes, F., Grover, O., Peterka, M., Seidl, J., Imrisek, M., Saarelma, S., Snyder, P., Sos, M., Caloud, J. COMPASS Upgrade: a high-field tokamak for ITER- and DEMO-relevant research. Nucl. Fusion, 64, 076028 (2024). https://doi.org/10.1088/1741-4326/ad4569

3 Houry, M., Aumeunier, M-H., Corre, Y., Courtois, X., Mitteau, R., Loarer, TH., Dubus, L., Gauthier, E., Gerardin, J., Gorse, V. Protection of the plasma facing components in the WEST tokamak, progress and development in view of ITER. Nucl. Fusion, 65, 016059 (2025). https://doi.org/10.1088/1741-4326/ad961b

4 Jain, J., Carrasco, M.F., Moreno, J., Davis, S., Pavez, C., Bora, B., Soto, L. Plasma-induced damage on the tungsten surface using a kilojoule plasma focus device: Applicable to study the damages on nuclear fusion reactor related materials. Phys. Plasmas, 31, 083510 (2024). https://doi.org/10.1063/5.0211839

5 Gao, B., Ding, R., Xie, H., Zeng, L., Zhang, L., Wang, B., Li, Ch., Zhu, D., Yan, R., Chen, J. Plasma-facing components damage and its effects on plasma performance in EAST tokamak. Fusion Engineering and Design Volume, 156, 111616 (2020). https://doi.org/10.1016/j.fusengdes.2020.111616

6 Kerkhof, S. Van den, Blommaert, M., Pitts, R.A., Dekeyser, W., Carli, S., Baelmans, M. Impact of ELM mitigation on the ITER monoblock thermal behavior and the tungsten recrystallization depth. Nuclear Materials and Energy, 27, 101009 (2021). https://doi.org/10.1016/j.nme.2021.101009

7 Guo, Z., Yu, B., Zhu, D., Xuan, Ch., Gao, B., Li, Ch., Ding, R., Chen, J., Du, Ch. Analysis of the transient heat flux on divertor surface during plasma disruption in EAST. Nuclear Materials and Energy, 36, 101503 (2023). https://doi.org/10.1016/j.nme.2023.101503

8 De Temmerman, G., et al. Data on erosion and hydrogen fuel retention in beryllium plasma-facing materials. Nucl. Mater. Energy, 27, 100994 (2021). https://doi.org/10.1016/j.nme.2021.100994

9 Jepu, I., Widdowson, A., Matthews, G.F., Coad, J.P., Likonen, J., Brezinsek, S., Rubel, M., Pintsuk, G., Petersson, P., Fortuna-Zalesna, E. Overview of damage to beryllium limiters by unmitigated disruptions and runaway electrons in the JET tokamak with metal walls. Nucl. Fusion, 64, 106047 (2024). https://doi.org/10.1088/1741-4326/ad6614

10 Pitts, R.A. Plasma-wall interaction impact of the ITER re-baseline. Nuclear Materials and Energy, 42, 101854 (2025). https://doi.org/10.1016/j.nme.2024.101854

11 Luo, Ch., Xu, L., Zong, L., Shen, H., Wei, Sh. Research status of tungsten-based plasma-facing materials: A review. Fusion Engineering and Design, 190, 113487 (2023). https://doi.org/10.1016/j.fusengdes.2023.113487

12 Wang, Sh., Li, J., Wang, Y., Zhang, X., Wang, R., Wang, Y., Cao, J. Thermal damage of tungsten-armored plasma-facing components under high heat flux loads. Sci Rep. 28;10(1), 1359 (2020). https://doi.org/10.1038/s41598-020-57852-8

13 Zhang, L., Zhang, X., Li, N., Zhang, P., Mei, X., Wang, Y., Uglov, V.V. Experimental and simulation studies on damage mechanisms of tungsten and molybdenum under compressed plasma flow irradiation. Nucl. Fusion, 63, 076010 (2023). https://doi.org/10.1088/1741-4326/acd016

14 Sattar, H., Jielin, Sh., Ran, H., Imran, M., Ding, W., Gupta, P.D., Ding, H. Impact of microstructural properties on hardness of tungsten heavy alloy evaluated by stand-off LIBS after PSI plasma irradiation. Journal of Nuclear Materials, 540, 152389 (2020). https://doi.org/10.1016/j.jnucmat.2020.152389

15 Kim, H.C., Bang, E., Kim, K-M., Oh, Ye., Han, H.N., Choi, J., Hong, S-H. Analysis of hardness and microstructural changes in Tungsten mono-blocks exposed to high heat flux at 10 MW/m^2. Fusion Engineering and Design, 170, 112530 (2021). https://doi.org/10.1016/j.fusengdes.2021.112530

16 Borovickaja, I.V., Pimenov, V.N., Masljaev, S.A., Demin, A.S., Morozov, E.V., Mihajlova, A.B., Serebrjanyj, V.N., Koljanova, A.S., Bondarenko, G.G., Gajdar, A.I., Matveev, E.V., Sasinovskaja, I.P. Osobennosti povrezhdaemosti poverhnostnyh sloev monokristallicheskogo vol’frama pod vozdejstviem moshhnyh impul’snyh potokov ionov gelija i plazmy. Russian Metallurgy, 4, 93–103 (2025). (in Russian). https://doi.org/10.31857/S08695733250493103

17 Wu, Z.M., Zhang, J., Zhang, J., Huang, J.C., Fan, Y., Yu, X.H., Zhao, Y.B., Zhu, J.L., Jin, C.Q., Wang, P., Fu, E.G. Nanocrystalline W-based alloys with ultrahigh hardness and exceptional irradiation tolerance. Nucl. Fusion, 59, 106050 (2019). https://doi.org/10.1088/1741-4326/ab34c8

18 Racz, A., Kun, P., Kerner, Z., Fogarassy, Z., Menyhárd, M. Tungsten Carbide Nanolayer Formation by Ion Beam Mixing with Argon and Xenon Ions for Applications as Protective Coatings. ACS Appl Nano Mater., 22;6(5), 3816–3824 (2023). https://doi.org/10.1021/acsanm.2c05505

19 Hou, Q-Q., Huang, K., Luo, L-M., Tan, X-Y., Zan, X., Xu, Q., Zhu, X-Y., Wu, Y-Ch. Microstructure and its high temperature oxidation behavior of W-Cr alloys prepared by spark plasma sintering. Materialia, 6, 2019, 100332 (2023). https://doi.org/10.1016/j.mtla.2019.100332

20 Dosbolayev, M.K., Tazhen, A.B., Ramazanov, T.S., Ussenov, Ye.A. Investigation of dust formation during changes in the structural and surface properties of plasma irradiated materials. Nucl. Mater. Energy, 33, 101300 (2022), https://doi.org/10.1016/j.nme.2022.101300

21 Dosbolayev, M.K., Tazhen, A.B., Kholmirzayev, A.N., Ussenov, Y.A., Ramazanov, T.S. Studies of the formation and distribution of cracks and various defects on the heated tungsten plate surface during pulsed plasma flux impact. Nuclear Materials and Energy, 37, 101540 (2023). https://doi.org/10.1016/j.nme.2023.101540

22 Tazhen, A.B., Dosbolayev, M.K., Ramazanov, T.S. Investigation of self-generated magnetic field and dynamics of a pulsed plasma flow. Plasma Sci. Technol., 24, 055403 (2011). https://doi.org/10.1088/2058-6272/ac5018

23 Dosbolayev, M.K., Tazhen, A.B., Ramazanov, T.S. Investigation and diagnostics of plasma flows in a pulsed plasma accelerator for experimental modeling of processes in tokamaks. Eurasian J. Phys. Functional Mater., 5, 198–210 (2021). https://doi.org/10.32523/ejpfm.2021050404

24 Tazhen, A.B., Dosbolayev, M.K., Pshikov, M.I., Usenov, E.A., Ramazanov, T.S. Measurement of the velocity of pulsed plasma flow at the PW-7 installation. Herald of the Kazakh-British Technical University, 2024;21(3), 273–280 (2024). (In Russ.) https://doi.org/10.55452/1998-6688-2024-21-3-273-280

25 Dosbolayev, M.K., Utegenov, A.U., Tazhen, A.B., Ramazanov, T.S. Investigation of dust formation in fusion reactors by pulsed plasma accelerator. Laser and Particle Beams, 35(4), 741–749 (2017). https://doi.org/10.1017/S0263034617000805

26 Qua, M., Konga, F., Yana, Sh., Uglov, V.V., Xue, J., Wang, Y. Damages on pure tungsten irradiated by compression plasma flows. Nuclear Inst. and Methods in Physics Research, B 444, 33–37 (2019). https://doi.org/10.1016/j.nimb.2018.12.050

27 Moldabekov, Zh.M., Zhukeshov, A.M., Gabdullina, A.T., Amrenova, A.U. Investigation of radiation effect on tungsten and molybdenum materials. International Journal of Mathematics and Physics, 14(2), 56-63 (2023). https://doi.org/10.26577/ijmph.2023.v14.i2.07

[1]*Тәжен Ә.Б.,
PhD, ORCID ID: 0000-0002-3277-2086,
*e-mail: Aigerim@physics.kz
[1]Холмирзаев А.Н.,
докторант, ORCID ID: 0009-0003-4108-0879,
e-mail: kholmirzayev.abdulla@gmail.com
[2]Үсенов Е.А.,
PhD, ORCID ID: 0000-0001-7903-8674,
e-mail: yerbolat@physics.kz
[1]Досболаев М.Қ.,
ф.-м.ғ.к., профессор, ORCID ID: 0000-0002-0724-1793,
e-mail: merlan@physics.kz
[1]Рамазанов Т.С.,
ф.-м.ғ.д., профессор, ORCID ID: 0009-0009-2301-1152,
e-mail: ramazan@physics.kz

[1]Ашық түрдегі ұлттық нанотехнологиялық зертхана, әл-Фараби атындағы ҚазҰУ, Алматы қ., Қазақстан
[2]Принстон плазма физикасы зертханасы, Принстон университеті, Принстон қ., АҚШ

ИМПУЛЬСТІ ПЛАЗМАНЫҢ ӘСЕРІНЕН АЛДЫН АЛА ҚЫЗДЫРЫЛҒАН ВОЛЬФРАМНЫҢ МИКРОҚАТТЫЛЫҒЫ МЕН МАССАСЫНЫҢ ӨЗГЕРУІН ЗЕРТТЕУ

Аңдатпа

Мақалада ұзақтығы шамамен 0,2 мс болатын импульстік плазма ағынының әсерінен бірінші қабырға мен диверторға негізгі кандидат материал болып табылатын алдын ала қыздырылған вольфрам нысанасының микроқаттылығы мен массасының өзгеруін сипаттайтын эксперименттік зерттеу нәтижелері келтірілген. Тәжірибелер энергия және қуат тығыздықтары шамамен 1,1 МДж/м^2 және 5,5 ГВт/м^2 болатын 13 импульстен тұратын сериялармен жүргізілді. Микроқаттылық HVS-1000B өлшегіші арқылы анықталды; нысананың массасы плазмалық әсерге дейін және кейін CPA225D жоғары дәлдікті таразының көмегімен өлшенді. Вольфрам нысанасының микроқаттылығы сәулеленудің максималды дозасында да (39 импульске дейін) айтарлықтай өзгеріссіз қалатыны және байқалған өзгеріс өлшеу қателігі шегінде болатыны көрсетілген, бұл беткі қабаттың құрылымдық тұрақтылығын көрсетеді. Сыртқы құрылымдық элементтер материалының ластануы мен қайта тұндыруынан туындауы мүмкін нысана массасының (31 мг-ға дейін) ұлғаюы тіркелді. Энергиядисперсиялық спектроскопия (ЭДС) талдауы нысананың бетіне қайта тұндырылған тозаңды бөлшектерінде Cu, Zn, Ni және C сияқты қарқынды сызықтардың барын анықтады. Нәтижелер бұл бөгде компоненттердің нысананың беттік морфологисына айтарлықтай әсер ететінін және вольфрамның зақымдану механизмдерін түсіндіру кезінде ескеру қажет екенін көрсетеді.

Түйін сөздер: импульстік плазмалық үдеткіш, плазмалық ағын, алдын ала қыздырылған вольфрам нысанасы, микроқаттылық, нысана массасы, нысананың элементтік құрамы.

[1]*Тажен А.Б.,
PhD, ORCID ID: 0000-0002-3277-2086,
*e-mail: Aigerim@physics.kz
[1]Холмирзаев А.Н.,
докторант, ORCID ID: 0009-0003-4108-0879,
e-mail: kholmirzayev.abdulla@gmail.com
[2]Усенов Е.А.,
PhD, ORCID ID: 0000-0001-7903-8674,
e-mail: yerbolat@physics.kz
[1]Досболаев М.К.,
к.ф.-м.н., профессор, ORCID ID: 0000-0002-0724-1793
e-mail: merlan@physics.kz
[1]Рамазанов Т.С.,
д.ф.-м.н., профессор, ORCID ID: 0009-0009-2301-1152,
e-mail: ramazan@physics.kz

[1]Национальная нанотехнологическая лаборатория открытого типа, КазНУ им. аль-Фараби, г. Алматы, Казахстан
[2]Принстонская лаборатория физики плазмы, Принстонский университет, г. Принстон, США

Аннотация

В статье представлены результаты экспериментального исследования изменений микротвердости и массы предварительно нагретой вольфрамовой мишени, основного материала-кандидата для первой стенки и дивертора, под воздействием импульсного плазменного потока с длительностью приблизительно 0,2 мс. Эксперименты проводились в виде серии из 13 импульсов при плотности энергии 1,1 МДж/м^2 и плотности мощности около 5,5 ГВт/м^2. Микротвердость измерялась с помощью твердомера HVS-1000B; масса мишени до и после воздействия плазмы измерялась с помощью прецизионных весов CPA225D. Показано, что микротвердость вольфрамовой мишени остается практически неизменной даже при максимальной дозе облучения (до 39 импульсов), а наблюдаемое изменение находится в пределах погрешности измерения, что свидетельствует о структурной стабильности поверхностного слоя. При этом зафиксировано увеличение массы мишени (до 31 мг), вероятно, вызванное загрязнением и повторным осаждением материала внешних конструктивных элементов. Анализ методом энергодисперсионной спектроскопии (ЭДС) выявил интенсивные полосы Cu, Zn, Ni и C в частицах пыли, повторно осажденных на поверхности мишени. Результаты показывают, что эти инородные компоненты оказывают существенное влияние на морфологию поверхности и должны учитываться при интерпретации механизмов повреждения вольфрамом.

Ключевые слова: импульсный плазменный ускоритель, плазменный поток, предварительно нагретая вольфрамовая мишень, микротвердость, масса мишени, элементный состав мишени.